Microfluid Nanofluid (2012) 13:637–643
DOI 10.1007/s10404-012-1003-x

RESEARCH PAPER

Diamagnetic particle focusing using ferromicrofluidics with a single magnet

Litao Liang · Xiangchun Xuan

Received: 13 March 2012 / Accepted: 11 May 2012 / Published online: 1 June 2012

Abstract Focusing particles into a tight stream is critical to many applications such as microfluidic flow cytometry and particle sorting. Current magnetic field-induced particle focusing techniques rely on the use of a pair of repulsive magnets, which makes the device integration and operation difficult. We develop herein a new approach to focusing nonmagnetic particles in ferrofluid flow through a T-microchannel using a single permanent magnet. Particles are deflected across the suspending ferrofluid by negative magnetophoresis and confined by a water flow to the center plane of the microchannel, leading to a focused particle stream flowing near the bottom channel wall. Such three-dimensional diamagnetic particle focusing is demonstrated in a sufficiently diluted ferrofluid through both the top and side views of the microchannel. As the suspended particles can be visualized in bright field, this magnetic focusing method is expected to find applications to label-free (i.e., no magnetic or fluorescent labeling) cellular focusing in lab-on-a-chip devices.

Keywords Microfluidics · Ferrofluid · Particle focusing · Magnetophoresis · Lab on a chip

1 Introduction

Focusing particles into a tight stream is usually a necessary step prior to counting, detecting, and sorting them (Xuan et al. 2010). As traditionally defined, particles can be focused in either two-dimension (normally horizontal direction) or three-dimension (both horizontal and vertical directions). A two-dimensional focusing is usually sufficient for continuous-flow particle sorters (Pamme 2007). For the application to flow cytometers, however, three-dimensional focusing is necessary in order to enhance the electrical or optical detection (Huh et al. 2005; Chung and Kim 2007; Godin et al. 2008). It can also suppress particle adhesions to microchannel walls.

A variety of particle focusing methods have been developed in microfluidic devices (Huh et al. 2005; Chung and Kim 2007; Godin et al. 2008; Xuan et al. 2010), among which sheath flow focusing may be the most common one. This method often requires complicated microfabrication and flow control in order to obtain a three-dimensional focusing (Fu et al. 2004; Tsai et al. 2008; Howell et al. 2008; Watkins et al. 2009). Sheathless focusing uses a force to manipulate particles laterally to their equilibrium positions, and can be further classified as active or passive depending on whether the force involved is externally applied or internally induced (Xuan et al. 2010). For active particle focusing, a variety of force fields including optical (Zhao et al. 2007), acoustic (Shi et al. 2008), and electric (Yu et al. 2005; Chu et al. 2009; Liang et al. 2010) forces have been demonstrated to focus particles in two- or three-dimension. This kind of approaches often requires expensive peripheral instruments and/or complex channel designs.

Passive particle focusing has been achieved using inertial microfluidics (Di Carlo 2009), which depends sensitively on the Reynolds number and requires a large amount of solution and a huge number of particles (Di Carlo et al. 2007; Bhagat et al. 2009, 2010). Insulator-based dielectrophoresis (iDEP) is another passive technique that has been demonstrated to pump and focus particles concurrently (Zhu and Xuan 2009a), which is, however, prone to

L. Liang · X. Xuan (✉)
Department of Mechanical Engineering, Clemson University, Clemson, SC 29634-0921, USA
e-mail: xcxuan@clemson.edu

fouling due to, for example, surface impurity (Voldman 2006) and Joule heating (Hawkins and Kirby 2010; Sridharan et al. 2011). Hydrodynamic filtration (Aoki et al. 2009) and hydrophoresis (Choi et al. 2008) have also been employed to focus particles passively, which require the use of a complex microchannel network or an in-channel obstacle array. Additionally our group has recently developed a passive electrokinetic method to focus particles in serpentine (Zhu et al. 2009; Church et al. 2009) and spiral (Zhu and Xuan 2009b) microchannels via curvature-induced dielectrophoresis(C-iDEP) (Xuan 2011). However, this method provides only a two-dimensional focusing in the width direction of long microchannels.

Only until recently has magnetic field been exploited to focus particles in microfluidic devices. As compared to other techniques, magnetic method is non-invasive and free of fluid heating issues (if permanent magnets are used) that accompany nearly all other ones, and is therefore well suited to handle bioparticles (Gijs 2004; Pamme 2006; Gijs et al. 2010; Nguyen 2012). Afshar et al. (2011) demonstrated a three-dimensional focusing of superparamagnetic particles by the use of a pair of asymmetrically arranged electromagnetic tips. The magnetic particles are first retained on one sidewall and then progressively released by lowering the current of an electromagnetic coil. The particle focusing is then realized by introducing a sheath flow to push the particles to the channel center.

The focusing of nonmagnetic particles has been obtained in paramagnetic solutions by Pamme's group (Peyman et al. 2009; Rodriguez-Villarreal et al. 2011) and in ferrofluids by Mao's group (Zhu et al. 2011a). Two repulsive magnets are used in both cases to create a magnetic field gradient null in the center of the microchannel, which, however, causes two difficulties in the operation. The first difficulty is to overcome the repulsion force and place the two magnets close enough for producing large magnetic field and field gradients in between. The second difficulty is to align the two magnets and keep them symmetric about the microchannel for controlling the position of the focused particle stream. To resolve these issues, Pamme's group (Peyman et al. 2009; Rodriguez-Villarreal et al. 2011) used a mechanical setup to precisely align two facing magnets about a fused silica capillary. This method is unsuitable for integration into planar lab-on-a-chip devices. Zhu et al. (2011a) embedded two long magnets into PDMS for an on-chip focusing, but the distance between them was 7 mm far. The result is a poorly focused stream (about 100 μm wide) of 5 μm particles. Moreover, as the tested ferrofluid is opaque, fluorescent particles must be used for visualization in their experiment (Zhu et al. 2011a).

In this paper, we develop a new approach to three-dimensional focusing of nonmagnetic particles in ferrofluid microflow with only a single permanent magnet. Since the magnet is embedded near the microchannel, the ferrofluid can be sufficiently diluted enabling a bright-field view of the focused particles in both the horizontal and the vertical planes. As such, fluorescent labeling of the suspended particles is not needed. The effects of ferrofluid flow rate and particle size on the particle focusing performance are examined.

2 Experiment

Figure 1a shows a picture of the microfluidic device used in our experiment. The T-shaped microchannel was fabricated in PDMS using a modified soft lithography technique (Liang et al. 2011; Zhu et al. 2012). A permanent magnet and a right-angle prism were embedded into PDMS and placed close to the microchannel for an enhanced magnetic field and the side-viewing of the particle motion, respectively. The microchannel consists of one 400 μm wide main-branch and two 200 μm wide side-branches with a uniform depth of 40 μm. Each branch is 10 mm long. The Neodymium-Iron-Boron (NdFeB) permanent magnet (B221, K&J Magnetics Inc.) is 600 μm away from the main-branch (edge-to-edge distance) and 3 mm from the side-branch. It has a dimension of $1/8'' \times 1/8'' \times 1/16''$ (thick) with the magnetization direction being perpendicular to the main-branch. The prism (N-BK7, Edmund Optics Inc.) is 500 μm away from the main-branch and 1 mm behind the magnet along the flow direction.

Fluorescent polystyrene particles (Duke Scientific Corp.) of 5 and 10 μm in diameter were re-suspended in 0.01× EMG 408 ferrofluid (Ferrotec Corp.) to a final concentration of 10^6–10^7 particles/ml. The dilution was prepared by mixing the original ferrofluid (1.2 % in volume magnetic nanoparticles) with a water-glycerol solution at a ratio of 1:99 in volume. The water-glycerol solution was prepared at the volume ratio of 7.8:2.2 in order to match the density of polystyrene particles (1.05 g/cm^3) (Liang et al. 2010). To drive the particulate and sheath flows, two identical pipette tips were inserted into the PDMS slab serving as the two inlet reservoirs. The outlet reservoir was emptied prior to experiment. As labeled in Fig. 1a, the particle solution in ferrofluid was introduced to the inlet reservoir that is closer to the magnet (i.e., on the same side as the magnet with respect to the main-branch). Meanwhile, an equal volume of water-glycerol solution (also 7.8:2.2 in volume to closely match the viscosity and density of the particle-suspending ferrofluid) was injected to the other inlet reservoir for obtaining an identical flow rate in the two side-branches. Particle motion was visualized and recorded using an inverted microscope (Nikon Eclipse TE2000U) equipped with a CCD camera (Nikon DS-Qi1Mc). The obtained images were processed using the Nikon imaging software (NIS-Elements AR 2.30).

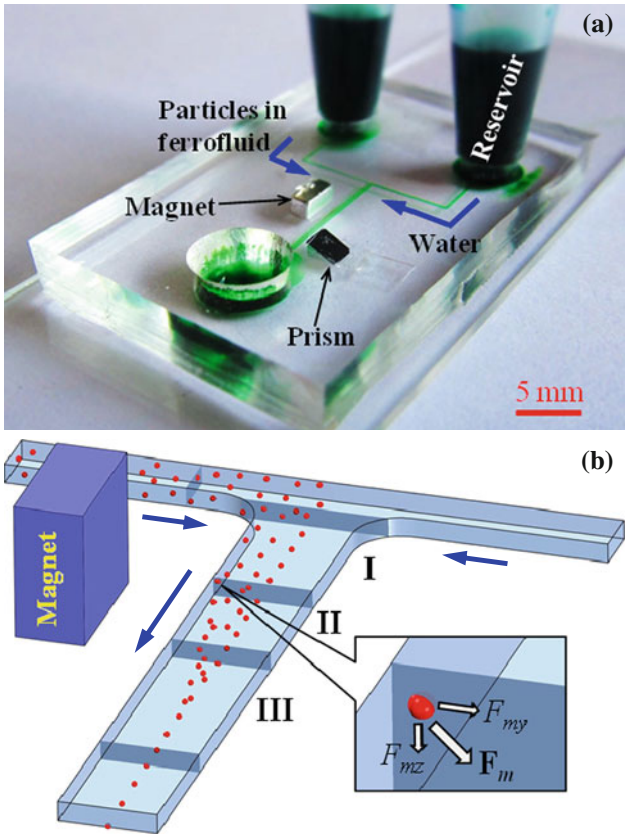

Fig. 1 **a** Picture of the microfluidic device used in the experiment; **b** schematic (not to scale) of the magnet-microchannel system illustrating the diamagnetic particle focusing mechanism. The labels I, II and III in **b** indicate the three view windows referred to in Figs. 2, 3 and 4. The *black arrows* indicate the particle/fluid flow directions

3 Theory

Nonmagnetic particles experience a negative magnetophoretic force, $\mathbf{F}_m$, in ferrofluid when subjected to a non-uniform magnetic field (Erb and Yellen 2009; Zhu et al. 2010, 2011b),

$$\mathbf{F}_m = -\mu_0 V_p (\mathbf{M}_f \cdot \nabla)\mathbf{H} \tag{1}$$

where μ_0 is the permeability of free space, V_p is the volume of the particle, $\mathbf{M}_f$ is the effective magnetization of the ferrofluid, and $\mathbf{H}$ is the magnetic field at the particle center. It is noted that in Eq. (1) the magnetization of nonmagnetic particles has been assumed negligible as compared to that of the ferrofluid, $\mathbf{M}_f$. The magnitude of the latter, M_f, is determined using the Langevin function, $L(\alpha)$ (Rosensweig 1985),

$$\frac{M_f}{\phi M_d} = L(\alpha) = \coth(\alpha) - \frac{1}{\alpha} \tag{2}$$

$$\alpha = \frac{\pi \mu_0 M_d H d^3}{6 k_B T} \tag{3}$$

where ϕ is the volume fraction of magnetic nanoparticles with a saturation moment, M_d, H is the magnetic field magnitude, d is the average diameter of the magnetic nanoparticles, k_B is the Boltzmann constant, and T is the ferrofluid temperature. Owing to the negative sign in Eq. (1), $\mathbf{F}_m$ is directed against the magnetic field gradient. Therefore, nonmagnetic particles are repelled away from the magnet (more specifically, the magnet center where the magnetic field achieves the maximum) and deflected across the ferrofluid in both the channel width and depth directions as indicated by the horizontal and vertical components of $\mathbf{F}_m$ in Fig. 1b. Such three-dimensional diamagnetic particle deflection has been recently demonstrated by the authors in a ferrofluid flow through a straight microchannel (Liang et al. 2011).

Since nonmagnetic particles experience a negligible magnetic force in water, the ultimate position of those three-dimensionally deflected particles in the main-branch of the T-microchannel is to follow the interface of the ferrofluid and sheath water in the horizontal plane and to flow right above the bottom channel wall in the vertical plane. This is achieved as long as sufficient residence time is available for particles to undertake the diamagnetic deflection inside the ferrofluid. As the 0.01× ferrofluid used in our experiment has approximately the same density and viscosity as those of water (note that both solutions were mixed with glycerol to obtain the desired density), an equal volume of these two fluids in the two inlet reservoirs is expected to produce a similar flow rate in the two side-branches. As such, the interface between the two co-flowing fluids should align with the center plane of the main-branch if diffusional mixing is considered slow and neglected. In other words, nonmagnetic particles are expected to exit the main-branch of the T-microchannel in a focused stream near the bottom edge of the center plane as schematically illustrated in Fig. 1b.

The effectiveness of such three-dimensional diamagnetic particle focusing is dependent on the particle deflections in both the horizontal and vertical planes, which are determined by the ratios of the particle speeds perpendicular and parallel to the flow (Liang et al. 2011; Zhu et al. 2012),

$$\text{Deflection}_i = \frac{U_{p,i}}{U_{p,x}} = \frac{U_{m,i}}{U_f + U_{m,x}} \approx \frac{U_{m,i}}{U_f} \quad (i = y, z) \tag{4}$$

where $U_{p,i}$ $(i = x, y, z)$ denotes the particle speed in the directions of fluid flow (x), channel width (y), and channel depth (z), respectively, $U_{m,i}$ is the magnetophoretic particle speed in each of the three directions, and U_f is the ferrofluid flow speed. Balancing the magnetic force, $\mathbf{F}_m$, in Eq. (1) with the Stokes drag force yields the magnetophoretic particle velocity, $\mathbf{U}_m$ (Liang et al. 2011),

$$\mathbf{U}_{\mathrm{m}} = \frac{\mathbf{F}_{\mathrm{m}}}{6\pi\eta a f_{\mathrm{D}}} = \frac{-\mu_0 \phi a^2}{9\eta f_{\mathrm{D}}} \frac{M_d L(\alpha) \nabla \mathbf{H}^2}{H} \quad (5)$$

where η is the ferrofluid viscosity, a is the radius of nonmagnetic particles, and f_{D} is the drag coefficient that is used to account for the particle–wall interactions (Happel and Brenner 1973). Neglecting the contribution of magnetophoresis to the x-direction particle velocity [see the approximation in Eq. (4)], one can see that the particle *deflection* and hence focusing increase with the rise of nonmagnetic particle size and magnetic nanoparticle concentration (i.e., the ferrofluid concentration) or with the reduction of ferrofluid speed.

4 Results and discussion

4.1 Demonstration of three-dimensional diamagnetic particle focusing

Figure 2 shows the top-view (a) and side-view (b) images of 5 μm nonmagnetic particles at the T-junction (Window I), magnet center (Window II), and 3 mm after the magnet (Window III) of the proposed ferromicrofluidic focuser; see Fig. 1b for the locations of the view windows. These images are each obtained by superimposing a sequence of more than 200 snapshot images and will be named streak images below. The top-view results include fluorescent (top row, with a weak background light illumination to visualize the channel edges) and bright-field (bottom row) streak images, which both clearly illustrate the particle motion. Therefore, fluorescent labeling is actually not needed for particles re-suspended in the diluted ferrofluid. The mean flow speed of the ferrofluid is 0.5 mm/s in the side-branch, and was estimated by tracking 3–5 particles each at five different locations over the width of the side-branch in the straight section and then fitting the measured particle speeds to the fluid velocity profile in a rectangular channel.

At the T-junction (see Window I in Fig. 2a), particles experience negligible magnetic force and thus cover uniformly one-half of the main-branch without noticeable deflections. When particles move past the magnet center (see Window II in Fig. 2a), apparent deflection toward the channel center plane is observed. However, particles are all confined by the sheath water and unable to cross the ferrofluid-water interface. A significant amount of magnetic nanoparticles is noticed to accumulate at the sidewall nearer to the embedded magnet, as highlighted by the dashed-lines in the top-view images in Window II. Moreover, the accumulated nanoparticles seem to disturb the ferrofluid/water co-flows and shift their interface slightly away from the channel center plane. This phenomenon can be mitigated by the use of a larger flow rate, where particle focusing can be maintained by reducing the channel width. In addition, the instability of the ferrofluid/water interface under a magnetic field (Wen et al. 2009, 2011) may contribute to the off-center deviation of the focused particle stream as well. This issue will be investigated in future studies. At 3 mm after the magnet (see Window III in Fig. 2a], 5 μm particles are focused to a less than 25 μm-wide stream flowing along the channel center plane. Note that the particle stream is 200 μm wide before the magnet, indicating a more than eightfold focusing in the horizontal plane in terms of particle stream width.

Side-view images were recorded through an embedded prism 1 mm before or after the magnet along the flow direction. Only the fluorescent streak images are illustrated in Fig. 2b. It is observed that before the magnet (Fig. 2b, left) 5 μm particles disperse uniformly in the suspension and spread nearly the entire channel depth. Moreover, they migrate through the microchannel at significantly non-uniform speeds, implying that the particles were moving at different depth levels. In contrast, all the particles travel adjacent to the bottom channel wall and form a tight bright stream after the magnet (Fig. 2b, right). Furthermore, their travelling speeds become nearly identical to each other, indicating a good particle focusing in the vertical plane.

4.2 Flow rate effect on diamagnetic particle focusing

By varying the injected ferrofluid and water volumes in the two inlet reservoirs, we examined the flow rate effect on diamagnetic particle focusing in the T-microchannel. Figure 3a compares the snapshot (left column) and streak (right column) images of 5 μm particles at the mean ferrofluid flow speed of 0.5 (top row), 1.0 (middle row), and 2.0 (bottom row) mm/s, respectively. As predicted in Eq. (4), increasing the ferrofluid flow speed reduces the particle focusing in the horizontal plane. Moreover, the measured particle stream width scales almost linearly with the inverse of the flow speed as demonstrated in Fig. 3b. We have also studied the 5 μm particle focusing in the vertical plane. A complete deflection of particles to the bottom channel wall is observed at all the three flow speeds tested above [cf. Fig. 4a]. This is because the deflection distance in the vertical plane (which is the 40 μm channel depth) is much smaller than that in the horizontal plane (which is the 200 μm half-width of the main-branch).

4.3 Particle size effect on diamagnetic particle focusing

Figure 4 compares the horizontal and vertical focusing of 5 μm (a) and 10 μm (b) nonmagnetic particles in the

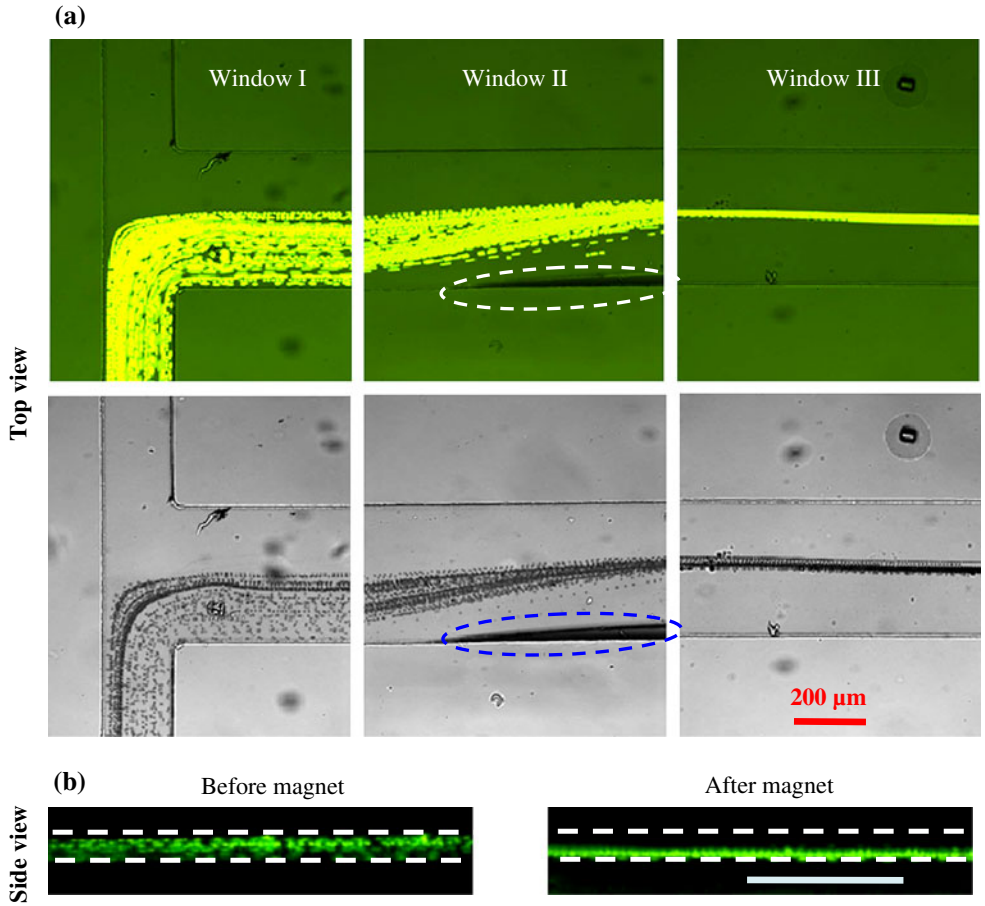

Fig. 2 Illustration of three-dimensional focusing of 5 µm nonmagnetic particles in ferrofluid flow through a T-microchannel using a single magnet: **a** *top-view* streak images (fluorescent in the *top row* and bright-field in the *bottom row*) in the three view-windows I, II and III (refer to Fig. 1b for the locations); **b** *side-view* streak images before (*left*) and after (*right*) the magnet. The mean flow speed of the ferrofluid in the side-branch is 0.5 mm/s. The *dashed lines* in **a** *highlight* the trapped magnetic nanoparticles on the sidewall that is nearer to the magnet. The *scale bar* in **b** represents 200 µm

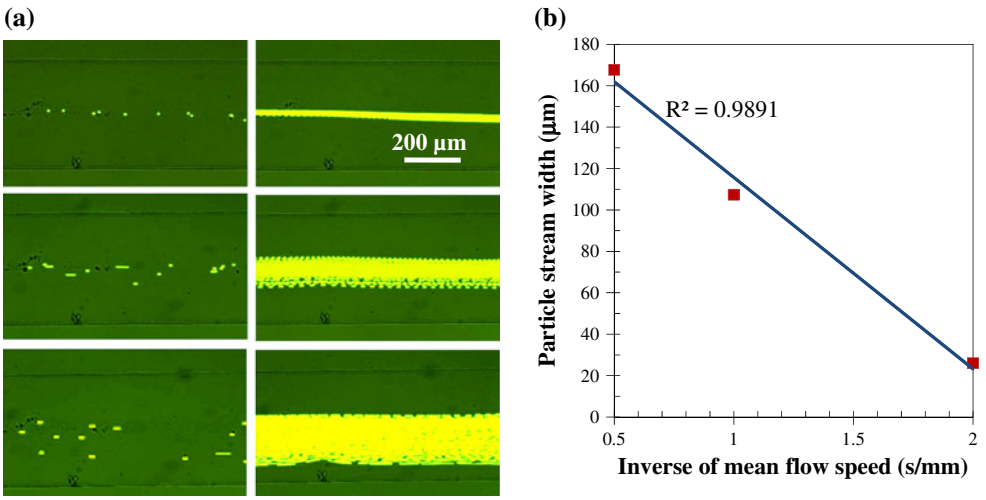

Fig. 3 Flow rate effect on the horizontal diamagnetic focusing of 5 µm particles in the T-microchannel: **a** snapshot images (*left column*) and streak (*right column*) images from Window III (see Fig. 1b) at the mean ferrofluid speed (in the side-branch) of 0.5 (*top row*), 1.0 (*middle row*), and 2.0 (*bottom row*) mm/s, respectively; **b** measured particle stream width (*symbols*) versus the inverse of mean ferrofluid speed. The *solid line* in **b** is a linear fit to the experimental data with the goodness of fit being indicated

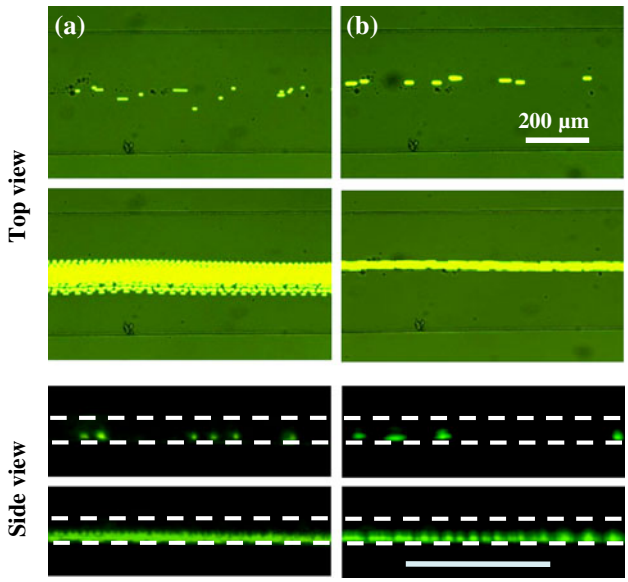

Fig. 4 Particle size effect on the horizontal (*top view*) and vertical (*side view*) focusing of 5 μm (**a**) and 10 μm (**b**) nonmagnetic particles in the T-microchannel at the mean ferrofluid flow speed of 1.0 mm/s. The *top* and *bottom* images in *each panel* are, respectively, the snapshot and streak images in Window III (see Fig. 1b). The *scale bar* in the *bottom-right* image represents 200 μm

T-microchannel through both the top-view and side-view images obtained in Window III. The mean ferrofluid flow speed in the side-branch is 1.0 mm/s for both cases. In the horizontal plane (see the top view images in Fig. 4), 5 μm particles form a stream of around 100 μm wide [refer to Fig. 3b]. In contrast, 10 μm particles travel through the main-branch in nearly a single file and form only a 20 μm wide stream along the channel centerline. This observation agrees with the quadratic dependence of magnetophoretic particle velocity on particle size; see Eq. (5). In the vertical plane (see the side-view images in Fig. 4), however, both 5 and 10 μm particles achieve a full-depth deflection and travel near the bottom channel wall. This is consistent with the observation in studying the flow rate effect, and is attributed to the much smaller channel depth than the width.

5 Conclusion

We have demonstrated a new magnetic approach to three-dimensional focusing of nonmagnetic particles using ferromicrofluidics with a single permanent magnet. The effects of ferrofluid flow rate and particle size on the particle focusing performance have been examined. It is found that the particle focusing effectiveness increases with increasing particle size and decreasing flow rate. Since ferrofluid is used to generate the magnetic "buoyant force", magnetic labeling is not needed for the suspended particles. Moreover, as the magnet is embedded into PDMS and placed close enough to the microchannel, the ferrofluid can be sufficiently diluted enabling a direct visualization of the suspended particles in bright field. As such, fluorescent labeling of particles is not needed, either. This demonstrated diamagnetic particle focusing is envisioned to find near-term applications to three-dimensional label-free (i.e., require neither magnetic nor fluorescent labeling) cellular focusing in lab-on-a-chip devices.

Acknowledgments This work was supported by NSF CAREER program under Grant CBET-1150670.

References

Afshar R, Moser Y, Lehnert T, Gijs MAM (2011) Three-dimensional magnetic focusing of superparamagnetic beads for on-chip agglutination assays. Anal Chem 83:1022–1029

Aoki R, Yamada M, Yasuda M, Seki M (2009) In-channel focusing of flowing microparticles utilizing hydrodynamic filtration. Microfluid Nanofluid 6:571–576

Bhagat AAS, Kuntaegowdanahalli SS, Papautsky I (2009) Inertial microfluidics for continuous particle filtration and extraction. Microfluid Nanofluid 7:221–230

Bhagat AAS, Kuntaegowdanahalli SS, Papautsky I (2010) Inertial microfluidics for sheath-less high-throughput flow cytometry. Biomed Microdev 12:187–195

Choi S, Song S, Choi C, Park JK (2008) Sheathless focusing of microbeads and blood cells based on hydrophoresis. Small 4:634–641

Chu H, Doh I, Cho Y (2009) A three-dimensional (3D) particle focusing channel using the positive dielectrophoresis (pDEP) guided by a dielectric structure between two planar electrodes. Lab Chip 9:686–691

Chung TD, Kim HC (2007) Recent advances in miniaturized microfluidic flow cytometry for clinical use. Electrophoresis 28:4511–4520

Church C, Zhu J, Wang G, Tzeng TJ, Xuan X (2009) Electrokinetic focusing and filtration of cells in a serpentine microchannel. Biomicrofluid 3:044109

Di Carlo D (2009) Inertial microfluidics. Lab Chip 9:3038–3046

Di Carlo D, Irimia D, Tompkins RG, Toner M (2007) Continuous inertial focusing, ordering, and separation of particles in microchannels. Proc Natl Acad Sci 104:18892–18897

Erb RM, Yellen B (2009) Magnetic manipulation of colloidal particles. In: Liu JP (ed) Nanoscale magnetic materials and applications, pp 563–590

Fu LM, Yang RJ, Lin C, Pan Y, Lee GB (2004) Electrokinetically driven micro flow cytometers with integrated fiber optics for on-line cell/particle detection. Anal Chim Acta 507:163–169

Gijs MAM (2004) Magnetic bead handling on-chip: new opportunities for analytical applications. Microfluid Nanofluid 1:22–40

Gijs MAM, Lacharme F, Lehmann U (2010) Microfluidic applications of magnetic particles for biological analysis and catalysis. Chem Rev 110:1518–1563

Godin J, Chen C, Cho SH, Qiao W, Tsai F, Lo YH (2008) Microfluidics and photonics for Bio-System-on-a-Chip: a review of advancements in technology towards a microfluidic flow cytometry chip. J Biophoton 1:355–376

Happel J, Brenner H (1973) Low Reynolds number hydrodynamics. Springer, Berlin
Hawkins BG, Kirby BJ (2010) Electrothermal flow effects in insulating (electrodeless) dielectrophoresis systems. Electrophoresis 31:3622–3633
Howell PB, Golden JP, Hilliard LR, Erickson JS, Mott DR, Ligler FS (2008) Two simple and rugged designs for creating microfluidic sheath flow. Lab Chip 8:1097–1103
Huh D, Gu W, Kamotani Y, Grotgerg JB, Takayama S (2005) Microfluidics for flow cytometric analysis of cells and particles. Physiol Meas 26:R73–R98
Liang L, Qian S, Xuan X (2010) Three-dimensional electrokinetic particle focusing in a rectangular microchannel. J Colloid Interf Sci 350:377–379
Liang L, Zhu J, Xuan X (2011) Three-dimensional diamagnetic particle deflection in ferrofluid microchannel flows. Biomicrofluid 5:034110
Nguyen NT (2012) Micro-magnetofluidics: interactions between magnetism and fluid flow on the microscale. Microfluid Nanofluid 12:1–16
Pamme N (2006) Magnetism and microfluidics. Lab Chip 6:24–38
Pamme N (2007) Continuous flow separations in microfluidic devices. Lab Chip 7:1644–1659
Peyman SA, Kwan EY, Margarson O, Iles A, Pamme N (2009) Diamagnetic repulsion—a versatile tool for label-free particle handling in microfluidic devices. J Chromatogr A 1216:9055–9062
Rodriguez-Villarreal AI, Tarn MD, Madden LA, Lutz JB, Greenman J, Samitier J, Pamme N (2011) Flow focusing of particles and cells based on their intrinsic properties using a simple diamagnetic repulsion setup. Lab Chip 11:1240–1248
Rosensweig RE (1985) Ferrohydrodynamics. Cambridge University Press, Cambridge
Shi J, Mao X, Ahmed D, Colletti A, Huang TJ (2008) Focusing microparticles in a microfluidic channel with standing surface acoustic waves (SSAW). Lab Chip 8:221–223
Sridharan S, Zhu J, Hu G, Xuan X (2011) Joule heating effects on electroosmotic flow in insulator-based dielectrophoresis. Electrophoresis 32:2274–2281
Tsai CG, Hou HH, Fu LM (2008) An optimal three-dimensional focusing technique for micro-flow cytometers. Microfluid Nanofluid 5:827–836
Voldman J (2006) Electrical forces for microscale cell manipulation. Annu Rev Biomed Eng 8:425–454
Watkins N, Venkatesan BM, Toner M, Rodriguez W, Bashir R (2009) A robust electrical microcytometer with 3-dimensional hydrofocusing. Lab Chip 9:3177–3184
Wen C, Yeh C, Tsai C, Fu L (2009) Rapid magnetic microfluidic mixer utilizing AC electromagnetic field. Electrophoresis 30:4179–4186
Wen C, Liang K, Chen H, Fu L (2011) Numerical analysis of a rapid magnetic microfluidic mixer. Electrophoresis 32:3268–3276
Xuan X (2011) Curvature-induced Dielectrophoresis (C-iDEP). The American Electrophoresis Society. http://www.aesociety.org/areas/curvature_induced_dep.php
Xuan X, Zhu J, Church C (2010) Particle focusing in microfluidic devices. Microfluid Nanofluid 9:1–16
Yu CH, Vykoukal J, Vykoukal DM, Schwartz JA, Gascoyne PRC (2005) A three-dimensional dielectrophoretic particle focusing channel for microcytometry applications. J Microelectromech Syst 14:480–487
Zhao Y, Fujimoto BS, Jeffries GDM, Schiro PG, Chiu DT (2007) Optical gradient flow focusing. Opt Express 15:6167–6176
Zhu J, Xuan X (2009a) Dielectrophoretic focusing of particles in a microchannel constriction using DC-biased AC electric fields. Electrophoresis 30:2668–2675
Zhu J, Xuan X (2009b) Particle electrophoresis and dielectrophoresis in curved microchannels. J Colloid Interf Sci 340:285–290
Zhu J, Tzeng TJ, Hu G, Xuan X (2009) Dielectrophoretic focusing of particles in a serpentine microchannel. Microfluid Nanofluid 7:751–756
Zhu T, Marrero F, Mao L (2010) Continuous separation of nonmagnetic particles inside ferrofluids. Microfluid Nanofluid 9:1003–1009
Zhu T, Cheng R, Mao L (2011a) Focusing microparticles in a microchannel with ferrofluids. Microfluid Nanofluid 11:695–701
Zhu T, Lichlyter DJ, Haidekker MA, Mao L (2011b) Analytical model of microfluidic transport of non-magnetic particles in ferrofluids under the influence of a permanent magnet. Microfluid Nanofluid 10:1233–1245
Zhu J, Liang L, Xuan X (2012) On-chip manipulation of nonmagnetic particles in paramagnetic solutions using embedded permanent magnets. Microfluid Nanofluid 12:65–73